

Breast-Specific Molecular Clocks Comprised of *ELF5* Expression and Promoter Methylation Identify Individuals Susceptible to Cancer Initiation



Masaru Miyano¹, Rosalyn W. Sayaman^{1,2}, Sundus F. Shalabi^{1,3}, Parijat Senapati⁴, Jennifer C. Lopez¹, Brittany Lynn Angarola⁵, Stefan Hinz¹, Arrianna Zirbes^{1,3}, Olga Anczukow⁵, Lisa D. Yee⁶, Mina S. Sedrak^{7,8}, Martha R. Stampfer⁹, Victoria L. Seewaldt¹, and Mark A. LaBarge^{1,7,9,10}

ABSTRACT

A robust breast cancer prevention strategy requires risk assessment biomarkers for early detection. We show that expression of *ELF5*, a transcription factor critical for normal mammary development, is downregulated in mammary luminal epithelia with age. DNA methylation of the *ELF5* promoter is negatively correlated with expression in an age-dependent manner. Both *ELF5* methylation and gene expression were used to build biological clocks to estimate chronological ages of mammary epithelia. *ELF5* clock-based estimates of biological age in luminal epithelia from average-risk women were within three years of chronological age. Biological ages of breast epithelia from *BRCA1* or *BRCA2* mutation carriers, who were high risk for developing breast cancer, suggested

they were accelerated by two decades relative to chronological age. The *ELF5* DNA methylation clock had better performance at predicting biological age in luminal epithelial cells as compared with two other epigenetic clocks based on whole tissues. We propose that the changes in *ELF5* expression or *ELF5*-proximal DNA methylation in luminal epithelia are emergent properties of at-risk breast tissue and constitute breast-specific biological clocks.

Prevention Relevance: *ELF5* expression or DNA methylation level at the *ELF5* promoter region can be used as breast-specific biological clocks to identify women at higher than average risk of breast cancer.

Introduction

Breast cancer is the most common cancer among women in the United States. There are many known risk factors for breast cancer including aging, obesity, alcohol consumption, tobacco

smoke, and family history (1, 2). Women who are germline carriers of pathogenic variants in *BRCA1* or *BRCA2* have approximately 70% risk of a breast cancer diagnosis by 80 years of age compared with only 10% risk of a breast cancer diagnosis in the general population (3). Ninety percent of women who receive a breast cancer diagnosis have no known inherited mutation (4) or family history (5), demonstrating the prevalence of sporadic breast cancer over inherited breast cancer. The fact that more than 75% of women diagnosed with breast cancer are over age 50 indicates that aging is the greatest risk factor for breast cancer, though we do not know the totality of molecular mechanisms underlying this relationship (6). There is considerable interest to identify factors that change with age to be used as biomarkers for estimating the risk of age-related diseases.

Age-specific DNA methylation patterns have been reported in a number of tissues (7–9). Horvath proposed that age-associated DNA methylation changes, so-called epigenetic clocks, can be used for estimation of biological age (10). Normal breast tissue adjacent to tumors showed poor correlation with Horvath's original pan-tissue epigenetic clock composed of 353 CpG sites (10), suggesting that breast may have a unique aging progression compared with other tissues. Age-dependent DNA methylation changes were reported in whole breast tissue at gene regulatory elements, at sites that show further alteration in cancer tissues (11, 12). We previously showed that DNA

¹Department of Population Sciences, Beckman Research Institute at City of Hope, Duarte, California. ²Department of Laboratory Medicine, Helen Diller Family Comprehensive Cancer Center, University of California, San Francisco, San Francisco, California. ³Irell and Manella Graduate School of Biological Sciences, City of Hope, Duarte, California. ⁴Department of Diabetes Complications and Metabolism, Beckman Research Institute at City of Hope, Duarte, California. ⁵The Jackson Laboratory for Genomic Medicine, Farmington, Connecticut. ⁶Department of Surgery, City of Hope National Medical Center, Duarte, California. ⁷Center for Cancer and Aging, City of Hope, Duarte, California. ⁸Department of Medical Oncology and Therapeutics Research, City of Hope National Medical Center, Duarte, California. ⁹Biological Systems and Engineering Division, Lawrence Berkeley National Laboratory, Berkeley, California. ¹⁰Center for Cancer Biomarkers, University of Bergen, Bergen, Norway.

M. Miyano and R.W. Sayaman contributed equally to this article.

Corresponding Author: Mark A. LaBarge, Population Sciences, City of Hope National Medical Center, 1500 E Duarte Road, Duarte, CA 91010. Phone: 626-218-0635; E-mail: mlabarge@coh.org

Cancer Prev Res 2021;14:779–94

doi: 10.1158/1940-6207.CAPR-20-0635

This open access article is distributed under the Creative Commons Attribution-NonCommercial-NoDerivatives 4.0 International (CC BY-NC-ND 4.0) license.

©2021 The Authors; Published by the American Association for Cancer Research

methylation and gene-expression patterns in luminal epithelial cells (LEp) shifted toward that of the myoepithelial lineage in an age-dependent manner (13, 14). The luminal-specific transcription factor *ELF5*, E74-like factor 5, stood out as a potential breast-specific aging biomarker because it exhibited excellent dynamic range of gene expression between LEps collected from average-risk younger (<30 y) and older (>55 y) women (13).

We hypothesized that measurements of *ELF5* expression or *ELF5* promoter methylation could be used to estimate chronological age of normal, non-cancer breast tissue. We examined RNA-sequencing and genome-wide DNA methylation in luminal epithelia from reduction mammoplasty tissue from women who are at average risk for breast cancer and showed that the expression of lineage-specific transcription factor *ELF5* was downregulated with age and negatively correlated with DNA methylation on its promoter region. In contrast, luminal epithelia from prophylactic mastectomy tissue from women with verified germline mutations that classify them as high risk for breast cancer, the acceleration of *ELF5* downregulation was detected in individuals with *BRCA1*, *BRCA2*, and *PALB2* mutations. We propose that the changes in *ELF5* expression or *ELF5*-proximal DNA methylation are emergent properties of at-risk breast tissue and constitute breast-specific biological clocks that could be used to identify women at higher than average risk of breast cancer.

Materials and Methods

Breast tissue collection and human mammary epithelial cells (HMEC) culture

Prophylactic mastectomy and contralateral to tumor breast tissues were collected at City of Hope (Duarte, CA) under approved Institutional Review Boards protocols, which included written informed consent. Breast organoids from reduction mammoplasty and peripheral-to-tumor breast tissues were collected in Dr. Stampfer's lab at Lawrence Berkeley National Laboratory (Berkeley, CA) with approved IRB protocols, which included written informed consent for tissue collection and sample distribution. Fourth-passage HMEC were generated and maintained according to previously reported methods using M87A medium containing cholera toxin and oxytocin at 0.5 ng/mL and 0.1 nmol/L, respectively (15, 16).

Flow cytometry

For dissociation of uncultured cells from organoids, organoids were digested with 0.5% trypsin/EDTA for 10 minutes at 37°C with agitation. After trypsin treatment, organoids were disrupted by vigorous shaking for 30 seconds. Then, cells were passed through 40 µm cell strainer (BD Falcon). Dissociated uncultured cells from breast organoids and fourth-passage HMEC were stained with anti-CD133-PE (BioLegend, clone 7) and CD271 (BioLegend, clone ME20.4) by following the standard flow cytometry protocol. Cells were sorted by AriaIII (Becton Dickinson).

RT-PCR for Gene-expression analysis

Total RNAs were isolated from FACS-enriched LEp and MEp with Quick-RNA Microprep kit (Zymo Research). For qPCR, cDNAs were synthesized with iScript reverse transcriptase (Bio-Rad) according to the manufacturer's manual. Quantitative gene-expression analysis was performed by CFX384 real-time PCR (Bio-Rad) with Universal SYBRGreen supermix (Bio-Rad). Data were normalized to RPS18 by relative standard curve method. For RNA-seq, isolated RNAs were submitted to Integrative Genomic Core at City of Hope (IGC at COH) for library preparation and sequencing. Primers are listed in **Table 1**.

RT-PCR analysis for isoform detection

RNA (400 ng) was reverse transcribed using Superscript III reverse transcriptase (Invitrogen). Semiquantitative PCR was used to amplify 10 ng cDNA with Phusion High-Fidelity DNA polymerase (NEB) at 56°C for 22 cycles (*GAPDH*) and 31 cycles (*ELF5*) with isoform-specific primers listed in **Table 1**. PCR products were separated in 1.8% agarose gel stained with SYBR Safe (Invitrogen) and imaged using ChemiDoc MP Imaging System (Bio-Rad). PCR bands were quantified using ImageLab 6.0 software (Bio-Rad). Bands were authenticated by Sanger sequencing (Eton Bioscience). Primers are listed in **Table 1**.

DNA methylation

Genomic DNA purifications from FACS-enriched each lineage were performed with Quick-gDNA Microprep kit (Zymo Research). Genomic DNA was digested with McrBC (New England BioLabs) and EcoRI (New England BioLabs), or EcoRI only as a control. DNA methylation was measured by real-time PCR using CFX384 (Bio-Rad). Amount of DNA methylation was normalized by internal primer control that targeted the DNA not containing CG dinucleotide. DNA methylation by McrBC method shows the percentage of cells with methylated DNA. For high-throughput DNA methylation analysis, purified gDNAs were submitted for sample preparation to UCLA Neuroscience Genomics Core and Integrative Genomic Core at COH for HumanMethylation450 and Human MethylationEPIC Beadchip array, respectively. Primers are listed in **Table 1**.

Luminal and myoepithelial RNA-sequencing data

RNA-sequencing preprocessing is fully described previously (14). Briefly, raw counts from FACS-sorted LEp and MEp were normalized and regularized log (rlog) transformed in DESeq2 package. Rlog values were batch-adjusted using *sva*'s ComBat function with the experimental design group as covariate in the model matrix. The experimental design group was defined by the combination of the culture condition (organoid, fourth passage), cell type (LEp, MEp), and age/risk status (average-risk young <30 y, average-risk old >55 y, and prophylactic mastectomy/contralateral/peripheral tissue to tumor without or with germline mutation) of the samples.

Table 1. Description of ssDNA oligo primers.

qRT-PCR	
RPS18	5'-GGGCGCGGAAAATAG-3'
RPS18	5'-CGCCCTCTGGTGAGGT-3'
ELF5	5'-TAGGGAACAAGGAATTTTCGGG-3'
ELF5	5'-GTACTACTAACCTTCGGTCAACC-3'
RT-PCR for isoform detection	
ELF5_ex1A_F1	5'-CTTGCCTTAAAAGCCTCCTC-3'
ELF5_ex5_R1	5'-ACAGTCTTGACTTTTGATGCCA-3'
GAPDH_F1	5'-AAGGTGAAGTCCGAGTCAACGG-3'
GAPDH_R1	5'-CCACTTGATTTGGAGGGATCT-3'
McrBC DNA methylation detection	
TIMP3	5'-TGTAATCCCACCCCTCTTG-3'
TIMP3	5'-GTTGGCCTTTCAGCAAGTTC-3'
ELF5	5'-GCGTGCAGTGAAAATAAAGAC-3'
ELF5	5'-CACACTGTATGTACCCTCATC-3'

Batch-adjusted rlog values were used for visualization of *ELF5* expression values. The mean rlog gene expression was calculated for individuals with replicate samples. For each of the 30,079 mapped transcripts, the mean rlog value from RM samples from each lineage and age group in fourth-passage HMEC (<30 y LEp/MEp $n = 11$, >55 y LEp/MEp $n = 8$) and organoids (<30 y LEp $n = 4$, <30 y MEp $n = 3$, >55 y LEp $n = 3$, MEp $n = 1$) was calculated and a linear regression between organoid and HMEC mean expression was plotted in (Fig. 1).

During quality control assessment, genes with low counts were determined using edgeR's filterbyExpr function with experimental design group and batch as covariates in the design matrix and were removed. Regression of batch-adjusted rlog values between cells isolated from organoid or fourth-passage culture was performed in each of the reduction mammoplasty LEp <30 y, LEp >55y, MEp <30 y, MEp >55 y subsets, and genes with absolute regression residuals ≥ 6 in either of the 4 subsets were considered outliers and flagged for exclusion. Normalization factors were calculated for the filtered raw count data using edgeR's calcNormFactors function. Genes with changes in lineage-specific expression (adj. $P < 0.1$) in young <30 LEp and MEp between organoid and fourth-passage culture were identified by differential expression analysis in the subset of average-risk reduction mammoplasty samples young <30 y LEp and MEp using limma's voom function with subject IDs used to calculate duplicate correlation and blocking, and design group and batch modeled in the design matrix. Genes with discordant expression between organoid and fourth-passage culture were subsequently excluded from lineage-specific and age-specific differential expression and downstream analysis of fourth-passage data. A final set of 17,328 genes were analyzed for differential expression.

Lineage-specific (young <30 y LEp vs. <30 y MEp) and age-dependent (young <30 y LEp vs. >55 y LEp) differential expression analysis in the subset of fourth-passage reduction mammoplasty LEps and MEps was conducted using limma's voom function as described (14). Subject IDs were used to calculate duplicate correlation and for blocking, and design group and batch were modeled in the design matrix. Moderated

statistics were computed using eBayes function in limma. P values were adjusted for multiple testing using Benjamini-Hochberg method. *ELF5* differential expression in <30 y and >55 y in fourth-passage LEps and MEps was obtained from (14). Statistical comparison of lineage-specific (young <30 y LEp vs. <30 y MEp) and age-dependent (young <30y LEp vs. >55y LEp) *ELF5* expression in reduction mammoplasty organoids was performed using a two-sided Welch t test.

Normal primary breast tissue gene-expression data

Normalized microarray expression data from normal primary breast tissue from 114 women (GSE102088, ≤ 30 y $n = 35$, >30 y <55 y $n = 68$, ≥ 55 y $n = 11$) (17) were downloaded from the Gene-Expression Omnibus (GEO) database using GEOquery package. *ELF5* expression in bulk tissue was obtained from this set.

Statistical comparison of expression of *ELF5* was performed across three age groups: young <30 y, middle aged >30 y <55y, and old >55 y using nonparametric Kruskal-Wallis test. Post-hoc analysis was performed using pair-wise Wilcoxon test comparing each age group, and P values were adjusted for multiple-testing across groups using Benjamini-Hochberg method.

TCGA RNA-sequencing data

RNA-sequencing FPKM-UQ values from TCGA were downloaded using TCGAbiolinks package. Analysis was restricted to samples from women with annotated PAM50 breast cancer subtype (PAM50 LumA $n = 566$, LumB $n = 207$, Her2 $n = 82$, basal $n = 194$, normal $n = 40$). *ELF5* $\log_2(\text{FPKM-UQ}+1)$ expression values in breast cancer tissue across PAM50 subtypes were obtained from this set.

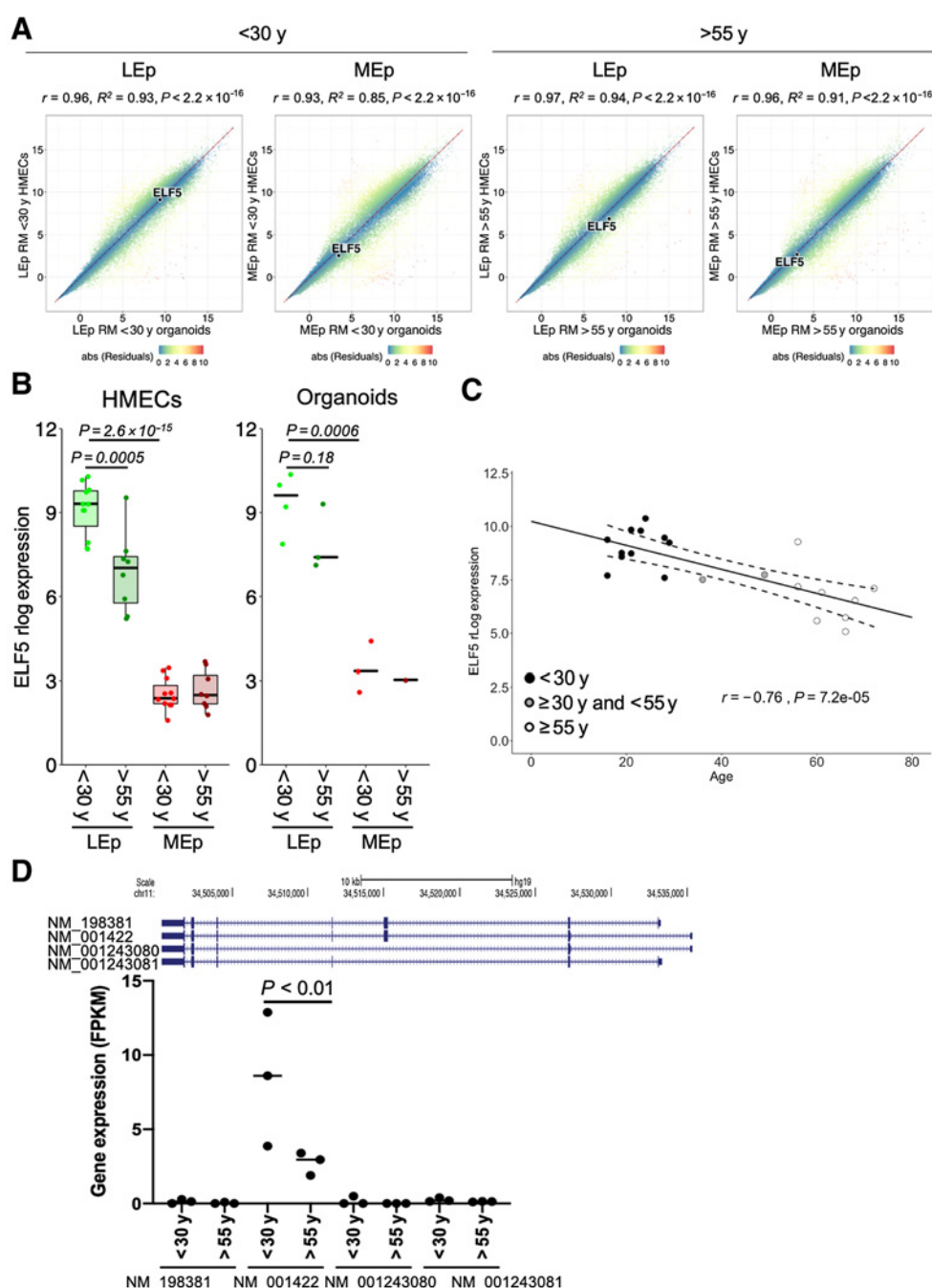
Statistical comparison of *ELF5* gene expression was performed across the five PAM50 subtypes: LumA, LumB, Her2, basal, and normal-like using nonparametric Kruskal-Wallis test. Post-hoc analysis was performed using pair-wise Wilcoxon test comparing each PAM50 subtype, and Wilcoxon P values were adjusted for multiple-testing using Benjamini-Hochberg method.

DNA methylation at the ELF5 locus in LEp

Illumina 450K array IDAT files preprocessing is fully described previously (14). Briefly, IDAT values were loaded, and detection P value filtering was conducted across the data set in ChAMP package. BMIQ normalization was performed, and DNA methylation m -values were calculated from beta-values using lumi package. The experimental design group was defined by the combination of the cell type and age group.

For visualization, DNA methylation m -values were batch-adjusted using sva's ComBat function with the experimental design group as covariate in the model matrix. Batch-adjusted m -values were converted to batch-adjusted beta-values in lumi, and were used to compare methylation levels of *ELF5* CpG sites across age/risk status and cell types.

Differential methylation of CpG sites was conducted in limma using filtered non-batch-adjusted m -values. Array

**Figure 1.**

ELF5 downregulation with age in both breast epithelial organoids and cultured HMEC. **A**, Linear regression plots of transcriptomes between organoids and HMEC in <30 y and >55 y LEP and MEp. X- and Y-axes show mean rlog values across subjects for 30,079 mapped transcripts from organoids ($n = 4 <30$ y, $n = 3 >55$ y LEP; $n = 3 <30$ y, $n = 1 >55$ y MEp) and fourth-passage HMEC ($n = 11 <30$ y, $n = 8 >55$ y LEP/MEp), respectively, for each lineage and age group. *ELF5* is indicated in each lineage and age group. Transcriptomes between organoids and HMEC are highly correlated in both lineages ($r = 0.96, P < 2.2e-16$ in LEP in <30 y, $r = 0.93, P < 2.2e-16$ in MEp in <30 y, $r = 0.97, P < 2.2e-16$ in LEP in >55 y, $r = 0.96, P < 2.2e-16$ in MEp in >55 y). **B**, Preserved *in vivo* lineage-specific (<30 y LEP vs. <30 y MEp) and age-dependent (<30 y LEP vs. >55 y LEP) *ELF5* expression in HMEC. Y-axis indicates regularized log (rlog) gene expression in box plots. *ELF5* is LEP-specific and the expression is downregulated with age in both organoids and HMEC. Differential expression (limma) adj. *P* values are shown for fourth-passage HMEC. Two-sided Welch *t* test *P* values are shown for fourth organoids. **C**, Linear regression of *ELF5* expression in LEP as a function of age. Y- and X-axes show rlog *ELF5* expression and age, respectively. Closed black, gray, and open circles show FACS-enriched LEP from >30 y, >30 y and <55 y, >55 y women, respectively. Pearson correlation coefficient is -0.76 and $P < 7.2e-5$, $n = 21$ ($n = 11, 2$, and 8 for <30 y, $\geq 30 \leq 55$ y, and >55 y, respectively). **D**, Isoform expression in LEP with age. Y-axis shows gene expression by FPKM counts. Chromosome location and gene structures in each isoform from UCSC genome browser are shown. Transcript variant 2 (NM_001422) is predominantly expressed in LEP and downregulated with age. All comparisons of <30 y NM_001422 across other isoform expressions in each age group show $P < 0.001$ except for the *P* value shown in D (Tukey multiple comparison test). $n = 3$ in each <30 y and >55 y age group.

weights were calculated, subject IDs were used to calculate duplicate correlation and for blocking, and design group and batch were modeled in the design matrix. Moderated statistics were computed using eBayes function in limma with trend applied. *P* values were adjusted for multiple-testing using the Benjamini–Hochberg method.

Normal primary breast tissue DNA methylation data

Illumina 450K array IDAT files from primary breast tissue were downloaded from two independent GEO data sets with 121 samples (GSE101961, ≤ 30 y $n = 38$, >30 y <55 y $n = 71$, ≥ 55 y $n = 12$); ref. 17) and 100 samples (GSE88883, ≤ 30 y $n = 36$, >30 y <55 y $n = 53$, ≥ 55 y $n = 11$; ref. 12), respectively. As with HMEC data, detection *P* value filtering and BMIQ normalization were performed in each data set. The experimental design group was defined by age groups (young <30 y, middle aged >30 y <55 y, and old >55 y). For visualization, DNA methylation *m*-values were calculated and batch-adjusted within each data set using ComBat with the experimental design group and BMI group as covariates in the model matrix. Batch-adjusted *m*-values were converted to batch-adjusted beta-values and were used to compare methylation levels of *ELF5* CpG sites in normal breast tissue across age groups.

Statistical comparison of DNA methylation of *ELF5* CpG sites was performed across Three age groups: young <30 y, middle aged >30 y <55 y, and old >55 y using nonparametric Kruskal–Wallis test. KW *P*-values were adjusted for multiple-testing across CpGs using Benjamini–Hochberg method. Post-hoc analysis was performed using pair-wise Wilcoxon test comparing each age group, and Wilcoxon *P* values were adjusted for multiple-testing using Benjamini–Hochberg method.

TCGA DNA methylation data

Normalized and processed beta-values from TCGA were downloaded using TCGAbiolinks package. Analysis was restricted to samples from women with annotated PAM50 breast cancer subtype and age at diagnosis (PAM50 LumA $n = 137$, LumB $n = 140$, Her2 $n = 43$, basal $n = 137$, normal $n = 34$). DNA methylation level (beta-values) of *ELF5* CpG sites in breast cancer tissue across PAM50 subtypes were obtained from this set.

Statistical comparison of DNA methylation of *ELF5* CpG sites was performed across the five PAM50 subtypes—LumA, LumB, Her2, basal, and normal-like—using nonparametric Kruskal–Wallis test. KW *P* values were adjusted for multiple-testing across CpGs using Benjamini–Hochberg method. Post-hoc analysis was performed using pair-wise Wilcoxon test comparing each PAM50 subtype, and Wilcoxon *P*-values were adjusted for multiple-testing using Benjamini–Hochberg method.

DNA methylation in high-risk LEp

DNA methylation measured using Infinium 450K Methylation and EPICMethylation BeadChips were analyzed using a

custom R script. The arrays were read and normalized using the minfi package, which return methylation *m*-values (18). 450k and EPIC array data were normalized by removal of batch effects using ComBat (19). Conversion of methylation beta-values from *m*-values were carried out using Lumi package. Methylation beta-values, which are an approximation of the percentage of methylation of a given CpG site, are calculated as the ratio of the methylated probe intensity and the overall intensity (sum of methylated and unmethylated probe intensities).

ELF5 DNAm multiple regression

A multiple linear regression DNAm age predictor was generated based on the *ELF5* DNA methylation beta-values in average-risk LEps of five CpGs selected based on their high correlation to chronological age and anticorrelation to *ELF5* expression (age \sim cg04504043 + cg11875459 + cg21017775 + cg11343506 + cg22731981). This *ELF5*-based multiple regression was used to predict the DNAm age of average-risk and high-risk LEps. A separate tissue-based multiple regression was generated based on the DNA methylation beta-values of the five selected *ELF5* CpGs in normal primary breast tissues from three public data sets: GSE101961 ($n = 121$; ref. 17), GSE88883 and GSE74214 ($n = 100$ and $n = 18$; ref. 12). For LEp and primary tissue, *ELF5*-based DNAm age was then plotted against chronological age, and linear regression R^2 , R , and *P* values were calculated.

Horvath clock

DNAm age was calculated for average-risk LEp and for each of three publicly available data sets of normal primary breast tissue from the Infinium 450K platform: GSE101961 ($n = 121$; ref. 17), GSE88883 and GSE74214 ($n = 100$ and $n = 18$; ref. 12) based on the 353 CpG Horvath pan-tissue clock (10) using the publicly available code (<https://horvath.genetics.ucla.edu/html/dnamage/>). Unfiltered and unnormalized DNAm beta-values were inputted as required. Data were normalized using BMIQ normalization as provided in the code. DNAm age was computed for each sample. Horvath clock predicted DNAm ages were averaged in average-risk LEp with replicate samples. For LEp and primary tissue, Horvath DNAm age was then plotted against chronological age, and linear regression R^2 , R , and *P* values were calculated. Error was calculated as the median absolute difference in biological and chronological age. Because the Horvath clock is not compatible with EPIC arrays, DNAm age of average-risk and high-risk LEp from the EPIC platform was not calculated.

MEAT DNAm clock

DNAm age was calculated for average-risk and high-risk LEp and for each of three publicly available data sets of normal primary breast tissue from either the Infinium 450K or EPIC platform: GSE101961 ($n = 121$; ref. 17), GSE88883 and GSE74214 ($n = 100$ and $n = 18$; ref. 12) using the Bioconductor MEAT package (<http://www.bioconductor.org/packages/>

release/bioc/html/MEAT.html). Unfiltered and unnormalized DNAm beta-values were inputted as required. Data were normalized using BMIQ normalization as provided in the code. DNAm age was computed for each sample. For LEp and primary tissue, MEAT DNAm age was then plotted against chronological age, and linear regression R², R, and P values were calculated. Error was calculated as the median absolute difference in biological and chronological age.

For LEp samples, the MEAT pipeline was adapted to allow for samples distributed across 450K and EPIC arrays to first be combined and ComBat batch-adjusted post-normalization and prior to DNAm age calculation. This was done to closely match the methodology we used in preprocessing and combining the LEp data from the two platforms. Briefly, 450K and EPIC data set were independently cleaned and calibrated using the MEAT pipeline. MEAT-generated normalized beta-values were then converted to m-values. Each data set was then ComBat batch-adjusted based on the chip IDs. Batch-adjusted m-values from 450K and EPIC arrays were then merged based on common probes across platforms. The merged data set was then further ComBat batch-adjusted based on platform type. Finally, the merged batch-adjusted m-values were converted back to beta-values and prepared for DNAm age prediction in MEAT. MEAT clock-predicted DNAm ages were averaged in average-risk LEp with replicate samples.

Ethical guidelines

The patient studies were conducted in accordance with the Declaration of Helsinki.

Results

ELF5 is downregulated as a function of age

To address whether age-associated *ELF5* expression in human breast can be used as an aging biomarker, we utilized primary HMEC derived from breast tissues of women who range in age from 16 to 72 years (Supplementary Table S1; refs. 15, 16, 20). Next-generation single-end RNA-sequencing (RNA-seq) was applied to examine transcriptomes in FACS-enriched CD133⁺/CD271⁻ LEps and CD133⁻/CD271⁺ myoepithelial cells (MEp; *n* = 43). Linear models of transcriptomes in LEp and MEp from reduction mammoplasty HMEC at fourth passage (*n* = 11 <30 y, *n* = 8 >55 y) and uncultured primary epithelial organoids (*n* = 4 <30 y, *n* = 3 >55 y LEp; *n* = 3 <30 y, *n* = 1 >55 y MEp) showed high correlation in both age groups (*r* = 0.96 *P* < 2.2e-16 in LEp in <30 y, *r* = 0.93 *P* < 2.2e-16 in MEp in <30 y, *r* = 0.97, *P* < 2.2e-16 in LEp in >55y, *r* = 0.96, *P* < 2.2e-16 in MEp in >55y; **Fig. 1A**). The magnitude of *ELF5* expression in both MEp and LEp was highly correlated between cultured HMEC and organoids (labeled in each plot). *ELF5* expression is LEp-specific and higher expression was detected in LEp from women who were <30 y compared with LEp from women >55 y in both HMEC and organoids (**Fig. 1B**). These data indicated that HMEC cultured in the M87A media (16) maintained lineage-specific and age-

dependent transcription profiles that are consistent with *in vivo*. *ELF5* expression level as a function of age showed negative correlation in LEp (*n* = 21, *r* = -0.76, *P* < 7.2 × 10⁻⁵; **Fig. 1C**), but not in MEp (*n* = 21, *r* = 0.089, *P* = 0.7; Supplementary Fig. S1A). *ELF5* shows tissue-specific isoform expression (21) so we next examined the possibility of age-dependent isoform expression in LEp. Expression levels of four *ELF5* transcript variants in HMEC were examined using paired-end RNA-seq (*n* = 3 <30 y, *n* = 3 >55 y). *ELF5* transcript variant 2 (Accession # NM_001422) had 34- to 62-fold higher expression than other isoforms (*P* < 0.001) and it was downregulated with age (*P* < 0.01; Supplementary Fig. S1B; **Fig. 1D**). This isoform was expressed in a lineage-specific manner independent of age. We confirmed predominant expression of transcript variant 2 and its age-dependence using semiquantitative RT-PCR method (*P* < 0.05; Supplementary Fig. S1B and S1C). Transcript variant 3 expression is lower, but the expression also appeared to be age dependent. Taken together, *ELF5* expression is strongly correlated with age in LEp from both cultured primary HMEC and uncultured organoids.

DNA methylation of the *ELF5* promoter is negatively correlated with age-dependent *ELF5* expression

ELF5 expression is regulated by DNA methylation on its promoter during mammary gland and embryonic development in mice (22, 23). RT-qPCR for *ELF5* transcript and a qPCR-based DNA methylation assay using a DNA methylation-dependent endonuclease, McrBC, were used to measure *ELF5* expression and DNA methylation in the *ELF5* promoter region. In LEp, methylation levels were positively correlated with age (**Fig. 2A**, black circles, *r* = 0.8824, *P* < 1E-4), and RNA levels were negatively correlated (**Fig. 2A**, light blue circles, *r* = -0.635, *P* < 0.05). In MEp, DNA methylation at the *ELF5* promoter was consistently high regardless of age and little transcript was detectable (**Fig. 2B**). The McrBC-qPCR method is not suitable for identifying specific single CpG dinucleotides. To identify age-associated differential methylation sites with single-nucleotide resolution, we utilized Illumina 450K DNA methylation arrays (*n* = 4 <30 y, *n* = 4 >55 y). The *ELF5* promoter and gene body regions were covered by 21 sequence-specific probes. Analyses of beta-values (ratio of the methylated probe intensity to overall intensity) showed 20 out of 21 loci were differentially methylated with age in LEp (BH adj. *P* < 0.05, with 17 out of 20 showing higher significance, BH adj. *P* < 0.001; **Fig. 2C**). Correlation of age and DNA methylation levels in each probe showed that probe cg19658620, cg04504043, cg02882375, cg22731981, and cg11875459 had high Pearson correlation coefficients (>0.918) and the errors [median absolute differences of chronological age and biological age by *ELF5* expression (1) were 4.4–5.6 years (**Fig. 2D**; Supplementary Table S2)]. DNA methylation and expression from the *ELF5* locus show striking lineage specificity in LEp versus MEp, and in LEp the age-dependent decrease in *ELF5* expression may be caused by increased promoter DNA methylation.

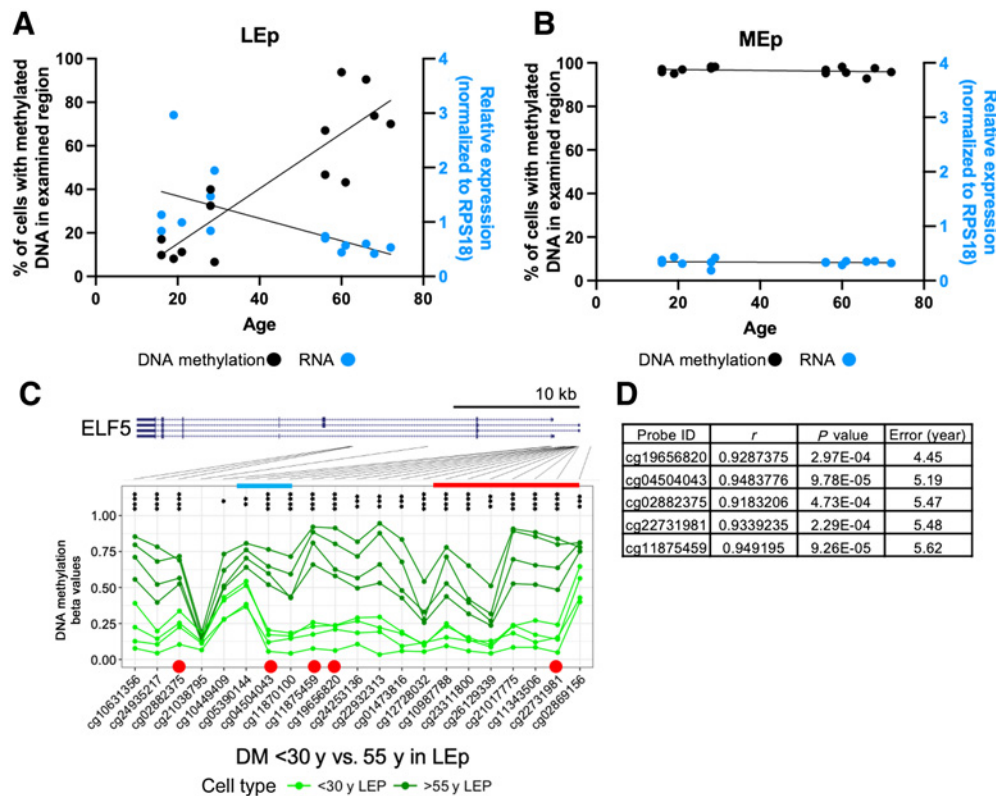


Figure 2.

DNA methylation in *ELF5* promoter region is negatively correlated to lineage-specific and age-dependent *ELF5* expression. Anticorrelation of DNA methylation to lineage-specific and age-dependent *ELF5* expression in LEP (A) and MEp (B). Left y-axis and right y-axis show percentage of cells with methylated DNA and *ELF5* gene expression, respectively. Black and light blue circles show DNA methylation and gene-expression plots, respectively. DNA methylation was measured by MspI digestion followed by qPCR. Gene expression was measured by qPCR, and data were normalized by RPS18 expression. Significances of differential gene expression and DNA methylation changes with age in LEP are < 0.001 (Mann-Whitney test). Not significant in MEp. $n = 14$ ($n = 7$ in each <30 y and >55 y age group) in both A and B. C, DNA methylation in *ELF5* region using Infinium 450K DNA methylation array ($n = 4$ <30 y, $n = 4$ >55 y). Differential DNA methylation states in each probe site are shown by beta-values of DNA methylation for <30 y (light green) and >55 y (dark green). Beta-values 0.0 and 1.0 indicate hypo- and hyper-DNA methylation, respectively. Chromosomal mapping of each CpG site is shown by solid lines below *ELF5* map from the UCSC genome browser. Promoter region in two major isoforms of *ELF5* is marked by red and light blue lines, respectively. Significance levels of differential methylation analysis (limma) adj. P values are denoted by asterisks: Benjamini-Hochberg, BH-adj. P : *, < 0.05 ; **, < 0.01 ; ***, < 0.001 ; ****, < 0.0001 . D, Linear regression of 450k DNA methylation array probes in the *ELF5* gene locus. Pearson correlation coefficient (r), P value, and error of five probes are summarized in table. Errors were calculated by median of absolute differences between biological age and chronological age. Corresponding genomic loci of the probes are shown by red dots in C.

Detection of age-related *ELF5* changes in bulk breast tissue

We examined DNA methylation and gene expression in publicly available data sets that were derived from whole breast tissue with the intent of extending our understanding of the robustness of this phenomenon. Utilizing the publicly available Illumina 450K DNA methylation array data sets (GSE101961, $n = 121$; and GSE88883, $n = 100$) from discarded reduction mammoplasty, we detected age-associated differential DNA methylation at the *ELF5* locus (Fig. 3A; refs. 12, 17). DNA methylation beta-values from younger (≤ 30 y) women were lower than those from middle age (>30 y, <55 y) and older (≥ 55 y) women. The baseline DNA methylation beta-values in the younger samples from the ensemble tissue data sets were higher than those from FACS-enriched LEP, suggesting the presence of more background signal from more abundant cell types. The decrease in beta-value dynamic range at CpGs in the

ELF5 locus from whole tissue can be seen more clearly when viewed as box plots of the individual probes (Fig. 3B), as compared with the range between age groups in FACS-enriched LEP (e.g., Fig. 2). Whereas the beta-values for the CpG island annotated cg11875459 in FACS-enriched LEP covered about 70% of the total range from younger to older, in bulk tissues we only detected changes of $<20\%$ of the total possible dynamic range with age.

We next asked whether age-dependent *ELF5* RNA expression was detectable in bulk tissues from a publicly available data set. The data set, GSE102088 ($n = 114$), was prepared from reduction mammoplasty and is composed of 33, 70, and 11 individuals who were younger (≤ 30 y), middle age (>30 y, <55 y), or older (≥ 55 y), respectively (17). Decreasing *ELF5* expression as a function of age was confirmed even in the whole tissue (Kruskal-Wallis $P < 0.001$) with significance of post-hoc pair-wise $P < 0.05$ and < 0.001 for younger versus middle age

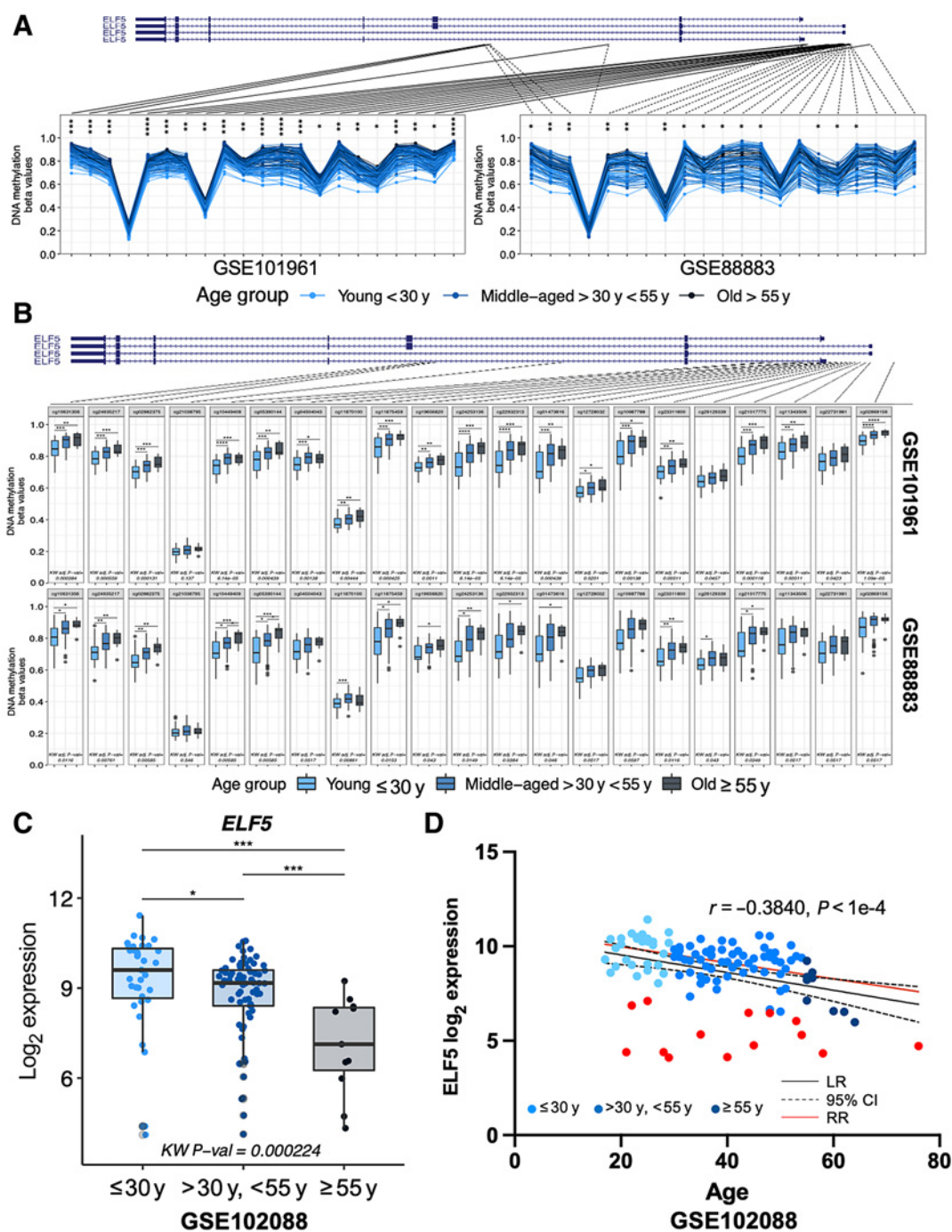


Figure 3.

Age-dependent *ELF5* expression and DNA methylation are detectable with bulk breast tissues. Age-dependent differential DNA methylation analysis in the *ELF5* gene locus with publicly available data sets of 450K DNA methylation array, GSE101961 ($n = 121$, ≤ 30 y $n = 38$, >30 y <55 y $n = 71$, ≥ 55 y $n = 12$) and GSE88883 ($n = 100$, ≤ 30 y $n = 36$, >30 y <55 y $n = 53$, ≥ 55 y $n = 11$), from reduction mammoplasty tissues are shown in **A** as line graph and in **B** as box plot. DNA methylations in the *ELF5* gene locus were increased with age in both data sets. Chromosomal mapping of each CpG site is shown by solid lines below *ELF5* map from the UCSC genome browser. Y-axis: DNA methylation beta-values. Kruskal-Wallis test adj. *P* value significance annotated in **A**, pair-wise post-hoc Wilcoxon test adj. *P* value significance annotated in **B**. Significance of differential DNA methylation change with age is denoted by asterisks: Benjamini-Hochberg, BH-adj. *P*: *, < 0.05 ; **, < 0.01 ; ***, < 0.001 ; ****, < 0.0001 . **C**, Age-dependent *ELF5* expression with publicly available data set, GSE102088, from reduction mammoplasty tissues ($n = 114$, ≤ 30 y $n = 35$, >30 y <55 y $n = 68$, ≥ 55 y $n = 11$). Kruskal-Wallis test *P* value annotated, pair-wise post-hoc, pair-wise post-hoc Wilcoxon test adj. *P* value significance annotated: *, $P < 0.05$; **, $P < 0.01$; ***, $P < 0.001$. **D**, Correlation plots with the same data set in **C**. $n = 114$, $r = -0.3840$, $P < 1e^{-4}$. Linear regression fit and 95% confidence intervals are shown in black solid and dashed lines, respectively. Robust regression is shown in the red line and outliers shown by the red circle are detected (14 out of 114). GEO data set accession numbers are shown in either bottom or left in each graph.

and for middle age versus older, respectively (Fig. 3C). Linear regression showed a weaker correlation between *ELF5* expression and age compared with FACS-enriched LEp (Fig. 3D, $r = -0.3840$, $P < 1E-4$). Robust regression, shown by a red line, revealed 12.3% outliers (14 out of 114; Fig. 3D, marked by red closed circles). The age-related changes in *ELF5* expression and DNA methylation beta-values in whole breast tissue are such that the publicly available data parallel our findings from FACS-enriched LEp.

CpG sites of the *ELF5* gene locus were not detected as age-associated CpGs in previous reports (12, 17). To compare with our findings, we examined three previously identified top age-associated CpGs from bulk tissue in our LEp data set (Supplementary Fig. S2). The two CpG sites (cg07303143 and cg06458239) also showed age-dependent increase of DNA methylation (Supplementary Fig. S2A), though the correlations were weaker than those with *ELF5* CpG in LEp, with MEp also contributing to the signal (Fig. 2C and D). However, cg01271695 on the *PXDN* gene locus showed poor correlation with age and DNA methylation in LEp in contrast to MEp (Supplementary Fig. S2B). The CpG cg01271695 has been identified to be negatively correlated to *PXDN* expression (12). We neither see age-dependent expression in MEp nor LEp. This difference could be due to the contribution of other cell types in the whole tissue context. We used FACS-enriched lineage-specific epithelial cells from HMEC that removed other cell types such as fibroblast and adipose cells in contrast to whole breast tissue preparations used in other studies. This illustrates the need for lineage-specific analysis to elucidate the age-dependent molecular changes that regulate cell type-specific function and that lead to cancer-predisposing dysregulation.

Relationship between age-related DNA methylation and luminal breast cancers

Luminal A and B breast cancer subtype incidence increases with age and comprise 80% of age-related breast cancers (24). Downregulation of *ELF5* in PAM50 Luminal subtypes compared with that in normal breast was reported (25) and we provide a confirmatory reanalysis from more than 1,000 women with the data generated by the TCGA Research Network in Fig. 4A. We next examined DNA methylation at the *ELF5* locus from more than 450 women across breast cancer subtypes in TCGA. DNA hypermethylation was more common in luminal A, luminal B, HER2, and normal PAM50 subtypes as compared with basal (Fig. 4B). DNA methylation levels in the *ELF5* gene body regions showed more DNA methylation than those in the promoter region. Accordingly, beta-values tended to be lowest in basal breast cancer (Fig. 4C). The higher DNA methylation states in luminal subtype breast cancers were not age-dependent. This suggests that age-dependent DNA methylation states at the *ELF5* locus could be a priming event for luminal subtype breast cancers, but that once cancer has set in, the relationship between age and *ELF5* expression or methylation ceases to exist.

ELF5 downregulation is accelerated in women with germline pathogenic *BRCA1* and *BRCA2* mutations

We next determined whether age-dependent changes in *ELF5* expression in LEp followed the same pattern in women at an average level of cancer risk and in women with clinically verified pathogenic germline mutations that significantly increase their lifetime risk for breast cancer. We enriched LEp by FACS from normal tissue of high-risk individuals who were verified to have germline mutations in *BRCA1*, *BRCA2*, or *PALB2*, and who ranged in age between 31 and 55 years (sample details in Supplementary Table S1). *ELF5* expression in high-risk LEp ($n = 12$) was decreased compared with younger (<30 y) average-risk women ($n = 21$; $P < 0.001$), and the magnitude of the decrease in expression was similar to that of older women (>55 y; Fig. 5A). Neither *BRCA1*, *BRCA2*, nor *PALB2* showed age-dependent differential expression in LEp from average-risk women (Supplementary Fig. S3A–S3C, respectively). Nor did *BRCA1*, *BRCA2*, or *PALB2* expression show any correlation with *ELF5* expression in LEp from average-risk women (Supplementary Fig. S3D–S3F, respectively). These data suggest that *ELF5* is not a direct target of *BRCA1*, *BRCA2*, or *PLAB2*, and vice versa.

We then asked whether normal epithelia from otherwise average-risk individuals diagnosed with breast cancer, but without a known pathogenic germline mutation, showed a decline of *ELF5* expression. Those samples, from eight discarded contralateral and two normal peripheral-to-tumor tissues, were examined from women who ranged in age from 25 to 72 y ($n = 10$). There was no difference in *ELF5* expression between LEp from tissue that was contralateral or peripheral to tumor and age-matched average-risk tissues, and overall the trends of *ELF5* expression tracked with age (Fig. 5A). We established a regression model with the average-risk LEp that showed *ELF5* expression is negatively correlated with age ($r = -0.76$, $P = 7.2e^{-5}$; Fig. 5B). Data from high-risk LEps were then fit to the average-risk regression and 92% (11 out of 12) high-risk LEp showed lower *ELF5* expression than would have been predicted at the same chronological age based on our model (Fig. 5B). Based on *ELF5* expression levels the biological ages of high-risk LEp would be predicted to be 11–42 years older than their chronological ages (Supplementary Table S3A). These results suggest that age-dependent decrease in *ELF5* expression is accelerated in epithelia from women with germline mutations that predispose them to breast cancer.

Next, we examined DNA methylation of the *ELF5* region in high-risk LEp ($n = 12$) with the Illumina EPIC platform (the updated version of 450K). Principal component analysis showed that DNA methylation levels around the *ELF5* locus in high-risk LEp were closer to those from average-risk older LEp and separated from those from average-risk younger LEp (Fig. 5C). We then built a multiple regression predictor of biological age based on the methylation levels of five *ELF5* probes in average-risk women. These five probes were selected based on their high correlation with age and anticorrelation with expression in LEp from average-risk

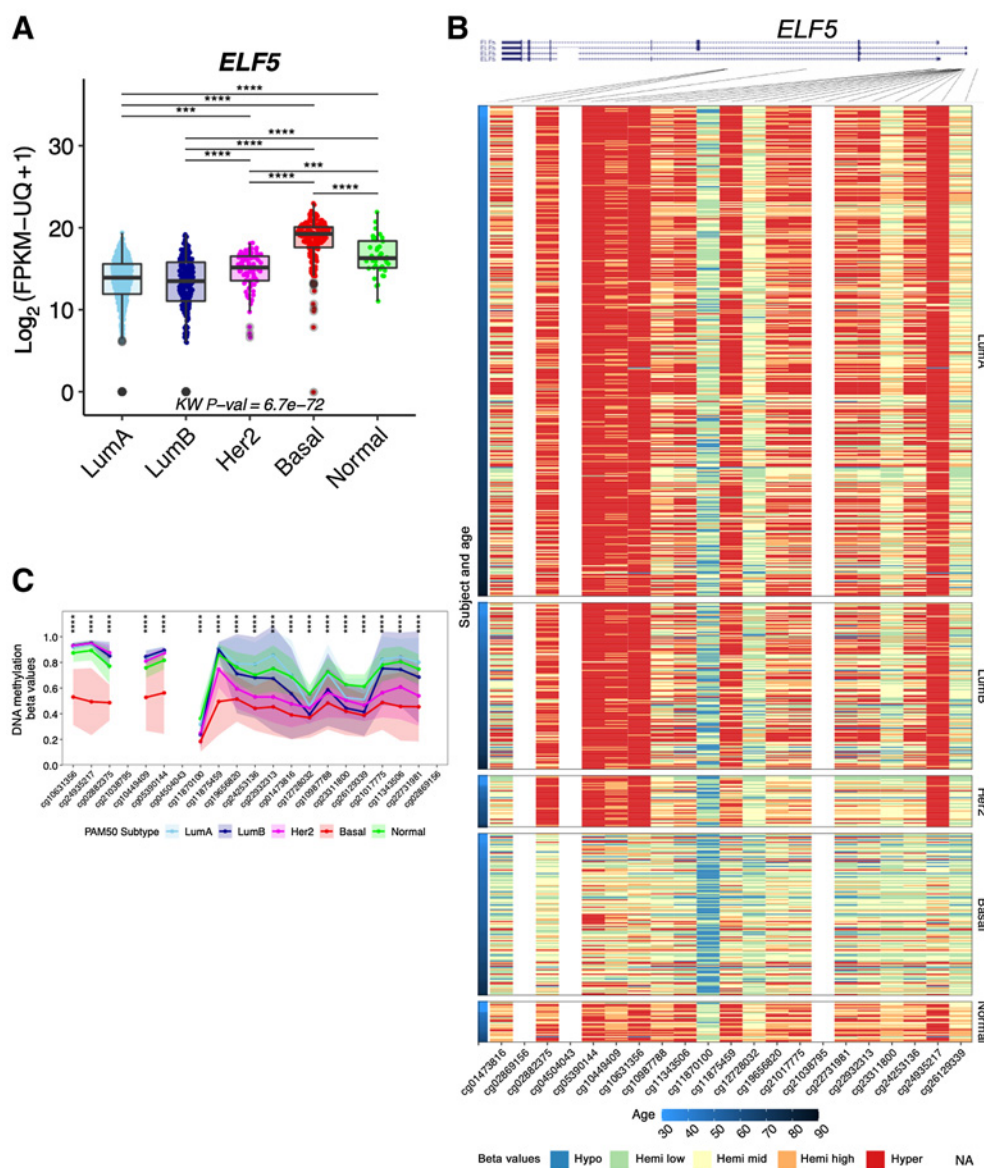


Figure 4. Breast cancer molecular subtype-specific *ELF5* expression and DNA methylation. *ELF5* expression (A) and DNA methylation status (B) of the *ELF5* gene locus with TCGA data set. ELF expression was lower in LumA, LumB, and Her2⁺ cancer subtypes, whereas the expression was higher in basal-like cancer compared with that in normal. DNA methylation states in the *ELF5* gene locus of each subtypes were negatively correlated to the *ELF5* expression. Breast cancer molecular subtypes are shown according to PAM50 classification. Color scales based on DNA methylation beta-values are shown below the heat map. Age is shown in the left of heat map. C, Differential DNA methylation in *ELF5* gene with PAM50 subtype. DNA methylation beta-values in each probe from every subtypes are superimposed. Chromosomal mapping of each CpG site is shown. Y-axis shows DNA methylation beta-values. Significance of differential DNA methylation change with age are denoted by asterisks: Benjamini-Hochberg, BH-adj. P: *, < 0.05; **, < 0.01; ***, < 0.001. LumA n = 566, LumB n = 207, Her2 n = 82, basal n = 194, normal n = 40 for *ELF5* expression data set. LumA n = 137, LumB n = 140, Her2 n = 43, basal n = 137, and normal n = 34 for DNA methylation analysis.

(Fig. 2D). The predicted biological ages of average-risk and high-risk women are shown in Supplementary Table S3B and are plotted against chronological age ($r = 0.99$, slope $m = 0.97$; Fig. 5D). Predicted age of 64% (9 out of 14) of the high-risk samples based on the multiple regression model shifted above the upper 95% confidence interval (CI), suggesting advanced biological age relative to chronological age. Individual linear regression models of DNA methylation

level of each of the five probes versus chronological age likewise show the majority of high-risk LEp are shifted above the 95% CI (Supplementary Fig. S4A). However, one or two high-risk samples in each probe were located below lower 95% CI that indicated younger biological age. For each sample, we calculated the absolute difference between chronological age and the predicted biological age from the average-risk multiple regression model. There is a

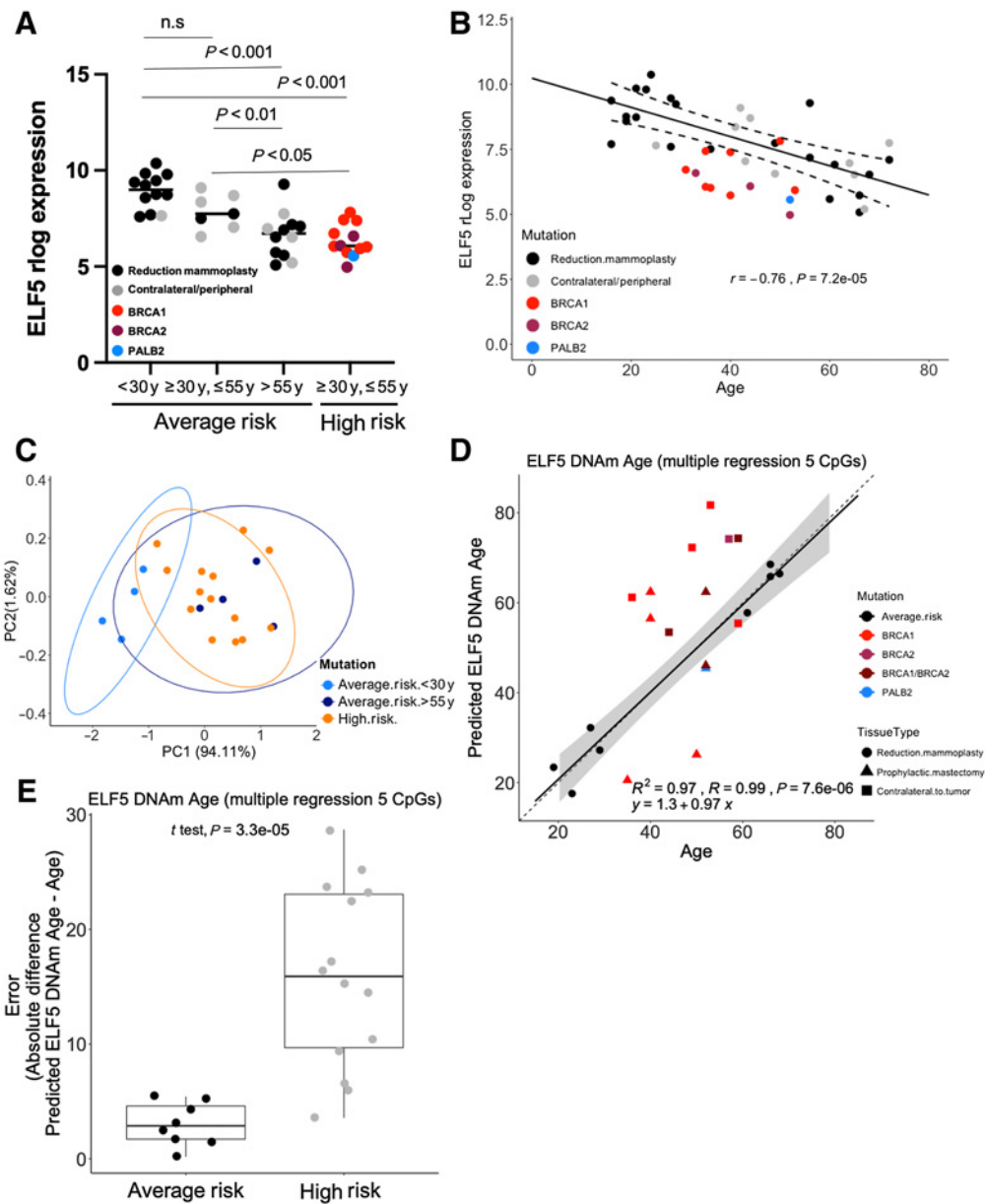


Figure 5.

Accelerated decline of *ELF5* expression and increased DNA methylation in high-risk women. **A**, Grouped dot plot showing *ELF5* expression in LEP from average-risk and high-risk women. Contralateral/peripheral are LEP derived from normal tissue that was contralateral or peripheral to a tumor. Y-axis shows rlog *ELF5* expression. *P* values by one-way ANOVA with Tukey multiple comparison test were shown above on the dot plots. $n = 43$ (average risk = 21, black dots; contralateral/peripheral = 10, gray dots; high risk = 12, red and blue dots). **B**, Linear regression of *ELF5* gene expression and chronological age. Solid line and dashed lines show regression fit and 95% CI, respectively. Mutation types in HR are indicated by colors indicated on the graph. $n = 43$ (average risk = 21, contralateral/peripheral = 10, and high risk = 12). **C**, Dot plot of the first two principal components based on the DNA methylation states of 21 probes in the *ELF5* gene locus. Each dot corresponds to an individual woman. Young or old from AR and HR women are shown by the colors indicated on the graph. $n = 22$ (Average Risk = 8 and high risk = 14). **D**, Predicted biological age of AR and HR based on a multiple regression generated with AR women based on the DNA methylation levels of 5 *ELF5* CpGs: cg19658620, cg04504043, cg02882375, cg22731981 and cg11875459. Predicted biological age is plotted against chronological age. Linear regression line with standard error is shown for AR women. Each point corresponds to an individual woman. $n = 22$ (Average Risk = 8 and high risk = 14). Tissue and Mutation types are labeled by different shapes and colors, respectively, as indicated on the graph. R square, correlation coefficient, *P* value and regression equation are shown in the graph. Diagonal with slope = 1 shown for reference. **E**, Comparison of errors between Average Risk and High-Risk women in predicted DNA methylation age. Errors (absolute difference between biological and chronological age) from the multiple regression based on the 5 *ELF5* probes are plotted *P* value is calculated by two-sided *t* test.

significantly greater error in high-risk LEp (error = 15.9 y) compared with average-risk (error = 2.9 y; Fig. 5E), which suggests increased variance in methylation at these sites is a property associated with cancer risk.

Because a majority of the high-risk samples did show significantly decreased *ELF5* expression, we examined the correlation of matched *ELF5* expression and DNA methylation in the high-risk LEp ($n = 7$) as a function of the five chosen probes (Supplementary Fig. S4B). These regression models indicated that 71%–86% of high-risk women tend to be outside of the 95% CI for any given regression compared with 0–25% of average risk. This suggests that the high-risk LEp may have decoupled the relationship between *ELF5* expression and methylation. Taken together, quantification of *ELF5* expression and DNA methylation can be used as biological clocks for human mammary epithelia. Moreover, biological age estimates relative to chronological ages of high-risk LEp showed increased variance relative to LEp from average-risk, further suggesting dysregulation of the LEp lineage in high-risk women. We hypothesize these *ELF5*-based clocks may be used to estimate breast cancer risk in a manner that is independent of the specific underlying monogenic risk factor.

Lastly, we compared how established DNAm clocks developed from bulk tissue predict biological age of isolated cell lineages. We applied the Horvath pan-tissue clock (10) to the average-risk LEp from the 450K array (the Horvath clock is not compatible with EPIC arrays). Likewise, we adapted the MEAT DNAm clock (26) with ComBat batch-adjustment post calibration to the average-risk and high-risk LEp data from the combined 450K and EPIC arrays. We found both clocks calculated DNAm ages of LEp samples with strong correlation to chronological age ($r = 0.96$, $r = 0.92$, respectively), but with a slope much less than 1 ($m = 0.65$ and $m = 0.51$, respectively), leading to high errors in predicting biological age in average-risk LEps (error = 8.3 y, error = 9.4 y, respectively) compared with the *ELF5*-based clock ($r = 0.99$, $m = 0.97$, error = 2.9 y; Supplementary Fig. S5A and S5B). Based on the linear regression of chronological versus biological age generated from average-risk LEp, the MEAT clock likewise predicts older biological ages in 8 of 14 high-risk LEp (error = 7.2 y; Supplementary Fig. S5B). The high error in age estimation suggests that whole tissue-based clocks are inadequate in capturing the age-dependent changes in the luminal lineage, and are susceptible to changes in composition of the breast. Indeed, differential age acceleration in LEp may partially explain why the Horvath clock was shown to be poorly calibrated in breast tissue with high error of 8.9 y in normal tissue ($cor\ r = 0.73$) and error of 13 y in normal adjacent to tumor ($cor\ r = 0.87$; ref. 10). We validated this finding using three publicly available data sets of normal primary breast tissue from the Infinium 450K platform: GSE101961 ($n = 121$; ref. 17), GSE88883 and GSE74214 ($n = 100$ and $n = 18$; ref. 12). Predicted biological ages of normal breast tissue recapitu-

lated previous results showing high error despite strong correlation with chronological age ($r = 0.88$, error = 12 y, and $r = 0.78$, error = 7.3 y, respectively) with the Horvath clock leading to an overestimate of biological age particularly in young women (Supplementary Fig. S5C and S5D). Moreover, multiple regression performed on the normal whole breast tissue based on DNA methylation of the five selected *ELF5* probes shows *ELF5*-based predicted biological age have weak correlation to chronological age ($r = 0.33$, error = 9.5 y; Supplementary Fig. S5E), likely due to contamination by other cell types that mute the *ELF5* signal from LEp. Together, these results indicate that biological age in breast tissue is complicated by many other factors, and a lineage-specific clock is needed to investigate the effects of age acceleration on individual cell types that may contribute differentially to aging-associated cancer initiation.

Discussion

The overwhelming majority of breast cancers are not attributable to monogenic germline risk factors, and may instead be attributed to polygenic, epigenetic, and/or environmental risk factors. There is a need to develop reliable tools for breast cancer risk assessment that will bolster early detection and prevention efforts. Here we show that *ELF5* is expressed in an age-dependent manner in normal whole breast tissue and in LEp, and that the changes in expression are due to changes in promoter methylation that also are age-dependent. In luminal subtype breast cancers, *ELF5* expression is exceedingly low concomitant with high levels of promoter methylation. Using average-risk epithelial cells to establish a model that relates chronological age to *ELF5* expression or methylation, we found that LEp from women with high-risk germline mutations in *BRCA1* and/or *BRCA2*, or *PALB2* show an accelerated aging phenotype based on *ELF5* expression and DNA methylation in the promoter-proximal region. We conclude from these data that *ELF5* expression and DNA methylation of its promoter constitute breast-specific aging biomarkers, or molecular clocks. We speculate that deviations from a model of chronological age based on *ELF5* expression or promoter methylation that is established from phenotypically normal average-risk breast will reveal a tissue's biological age. We hypothesize that significant deviation of biological age from chronological age is a property of tissue that is more susceptible to cancer initiation.

A number of molecular markers have been proposed for breast cancer risk assessment. Concentration of IGF-1 or sex hormones such as estradiol and testosterone in blood is associated with breast cancer risk (27, 28). The relationship between risk and IGF-1 concentration is detected only in premenopausal women and there is no standardized method to measure blood levels of IGF-1. The risk assessment by concentration of sex hormones is suitable for postmenopausal women, but not for all ages. Shortening of telomere length with age has been reported (29), and cancers have short telomeres, but a strong case cannot be made that age-dependent shortening occurs in

normal breast epithelia (30). Telomerase activity in normal cells is lower than that in cancer cells, but it would be challenging to detect quantitatively with limited sample quantity. Thus, telomere length and telomerase activity are not good candidates for breast cancer risk assessment. The relationship between DNA methylation and aging has been well discussed (7, 8, 31). Epigenetic clocks (DNA methylation age) have been proposed to estimate biological age by Horvath and others (9, 10, 32–34). The pan-tissue clock uses 353 CpG sites to estimate biological age in a number of tissues and showed an association between estimated biological age with a number of age-related diseases; however, the pan-tissue clock was poorly calibrated in predicting biological age of breast tissue leading to high errors (median absolute difference between biological chronological age) despite high correlation values (10). We found a similar magnitude of error between biological and chronological age despite high correlation values when we applied both the Horvath and MEAT clocks (another established bulk tissue-based DNAm age predictor) to 239 normal primary breast tissue from 3 publicly available data sets (12, 17). This suggests that biological age in breast tissue is complicated by other factors including changing breast composition and hormone profiles. Breast-specific epigenetic clocks were developed that predicted accelerated biological age in luminal breast cancers relative to normal tissue (11, 35). Aging changes overall breast tissue composition such that adipose increases, connective tissue decreases, and proportions of MEp decrease relative to an increase of LEp and epithelial progenitors in the epithelia (20). An example of the effect of these compositional changes was embodied by our observation that the dynamic range of *ELF5* gene expression and methylation changes with age was as much as 5-fold greater in purified LEp than in whole breast tissue. Indeed, the tissue-based clocks were not suited to predict biological age of LEp or to capture age-dependent changes in the luminal lineage. Lineage-specific age acceleration and its impact on cancer initiation may therefore be better measured by clocks developed specifically for a given cell type. Further studies will help to establish whether the estimated biological ages by the *ELF5* clock is due to changes in DNA methylation or other tissue components with age.

Random periareolar fine-needle aspiration (RPFNA) or ductal lavage (DL) are minimally invasive clinical techniques for obtaining small amounts of breast tissue to assess breast cancer risk in asymptomatic women who are suspected of being at increased risk due to germline inherited risk factors or family history (36). Materials obtained by either method can capture mixtures of epithelial, fibroblast, endothelial, adipose, and immune cells (although DL is highly enriched for sloughed off epithelial cells). We confirmed age-associated *ELF5* expression and DNA methylation was measurable even from normal whole breast tissue. This is important, because it seems likely that specimens collected by RPFNA and DL will be amenable to *ELF5* analysis, thus helping to pave the way for testing in a translational setting. From publicly available data derived from whole tissue, we observed that 12% (14 in 114) of women

showed significantly lower *ELF5* expression compared with what would have been predicted by chronological age—breast cancer incidence in the United States is ~13%. We were unable to obtain follow-up information on the patients embodied in the GSE102088 data set, but it is tempting to speculate that it may be possible to identify the minority of women who are at highest risk (independently of known genetic risk factors) based on regulation of *ELF5* in breast.

Tools are needed to identify and predict vulnerable subgroups at risk for developing breast cancer. Measures of biological age by the *ELF5* clock represent a potential way to assess emergent properties of the aging process that are linked to increased breast cancer risk. The ability to advance knowledge of the effects of aging on cancer has been constrained by a paucity of an agreed-upon biological measure or a combination of biological measures of aging that are sensitive or specific enough to accurately assess the physiologic aging process (37–40). Biomarkers that are currently available are unable to precisely measure an older individual's physiologic or functional age. However, in the future, biomarkers such as the *ELF5* clock, in combination with clinical aging assessments like the geriatric assessment (41–44), could enhance our understanding of how these factors interact and contribute to cancer risk. Although measures of biological aging are still in their infancy, they demonstrate translational promise to better understand biological aging in humans, and more research is needed to develop and validate these tools.

Downregulation of *ELF5* in non-human primate mammary glands occurs from the adult luteal to the postmenopausal stage (45), suggesting that downregulation of *ELF5* is conserved as an aging mechanism. Accelerated *ELF5* downregulation may be a sign of accelerated aging in breast tissue, indicating greater than average susceptibility to cancer initiation. *ELF5* expression is lower in luminal A and B breast cancer subtypes than in normal tissue (25), and *ELF5* downregulation was reported in all stages of cancer progression including atypical ductal hyperplasia, ductal carcinoma *in situ*, and invasive ductal carcinoma (46). We also observed decreased *ELF5* levels and sites with increased DNA methylation in the *ELF5* locus in luminal A and B breast cancer subtypes, which are strongly age-associated cancers. We do not know whether *ELF5* downregulation with age is a cause or a consequence of breast tissue aging. *ELF5* is a transcription factor and regulates stem/progenitor cell-fate decisions in mammary gland development (47). Dysregulation of *ELF5* affects the expression of downstream target genes in epithelial cells including *ESR1* and *FOXA1* (13, 25). In triple-negative breast cancer (TNBC), *ELF5* seems to work as tumor suppressor to inhibit epithelial-mesenchymal transition by suppressing *SNAI2* (48) and loss of *ELF5* enhances *IFNGR1* expression that leads to tumor growth and metastasis (49). Thus, decline of *ELF5* expression affects transcriptome networks that are associated with breast cancer progression and subsequently could affect cellular function in a way that increases susceptibility to cancer initiation though we do not yet know the mechanism.

The *ELF5* expression clock was generally consistent in identifying high-risk LEp by their accelerated decrease in expression relative to the model predicted by average-risk LEp. In contrast, the direction of change in methylation at any of the five CpG in high-risk samples was not consistent. Any given high-risk sample showed a change consistent with accelerated aging in only a subset of the five CpG islands that we evaluated for the clock (based on either the CpG-specific linear models or the multiple regression combining these CpGs). Indeed, the characteristic that distinguishes high-risk and average-risk samples according to the *ELF5* methylation clock is increased variation in the methylation levels across the five selected CpG sites in the high-risk samples. Because control of *ELF5* transcription is a composite outcome of the states of multiple promoter-proximal CpG sites, it may not be surprising that changes in transcription were mainly in one direction. Comparing the expression and methylation clocks in their ability to distinguish the high-risk samples, we identified 92% of high-risk samples with the gene-expression model and 64.3% of high risk with the gene methylation model.

Age-related gene expression in breast is reported to be influenced by hormone changes (50). *ELF5* was downregulated in the high-risk tissues regardless of age in our data set, thus even in women who were young and premenopausal. This suggests that decreased *ELF5* expression and changes in DNA methylation are more specifically related to aging and tissue-level changes that presage cancer susceptibility, in a manner that may not be dependent on hormone changes. Reported age-related genes such as *ESR1* or *FOXA1* are direct target genes of *ELF5* (25). We have reported that aging phenotypes in LEp are imposed by age-dependent cellular microenvironments (13). Therefore, estrogen signaling alone seems insufficient to explain the alteration of gene expression in breast as a function of age. We do not exclude the possibilities that *BRCA1*, *BRCA2*, and *PALB2* directly regulate *ELF5* expression, though our data suggested no correlation. Both *BRCA1* and *ELF5* gene products reportedly repress ER α activity through different mechanisms (25, 51). Accumulation of progenitors with more basal- or MEp-like features seems to be a phenotype in common among breast tissue of *BRCA1*-mutant (*BRCA1*^{mut}) carriers, *ELF5*-deficient mouse mammary glands, and breast tissue from older women (20, 47, 52). Thus, *BRCA1*^{mut} carriers may share a mechanism also present in *ELF5*-downregulated breast tissue from older women.

BRCA1^{mut} carriers and younger women tend to develop TNBC (24, 53), whereas aging is mainly related with luminal subtype breast cancers. *BRCA2*^{mut} carriers tend to develop luminal B subtypes. *PALB2*^{mut} carriers show higher rates for both luminal and TNBC subtypes (54), and this is perhaps due to the features of *PALB2* that interact with *BRCA1* and *BRCA2* (55). *ELF5* expression and *ELF5* DNA methylation clocks can be used to detect accelerated aging in both average-risk and high-risk women. However, *ELF5* expression tends to be higher and DNA methylation is lower in TNBC compared with luminal subtypes breast cancers. This suggests that the

regulation of *ELF5* gene in normal and cancer cells does not have the same mechanism, or that the difference between subtype may reflect cell of origin. Reactivation of *ELF5* expression by an unknown mechanism has been reported after tumors acquired drug resistance to tamoxifen (25, 56), again underscoring that *ELF5* regulation is likely quite different in the normal or cancer contexts.

The cell of origin of TNBC from *BRCA1*^{mut} carriers is thought to be cKIT⁺ luminal progenitors (52). Luminal progenitors may also be cell of origin of luminal subtype breast cancers (57). It has been reported that *BRCA1*^{mut} carriers increase *SNAI2* expression that inhibits luminal lineage commitment (58). *BRCA1* does not directly regulate *SNAI2* transcription; however, *BRCA1* seems to contribute to stabilization of the *SNAI2* gene product, the SLUG protein. Our data showed that *ELF5* expression was downregulated in *BRCA1*^{mut} carriers, and Chakrabarti and colleagues showed that *ELF5* suppressed Slug expression (48). This might be a potential mechanism relating to the susceptibility to develop TNBC in *BRCA1*^{mut} carriers. However, a recent study indicates that the intrinsic states of each epithelial lineage have dominant contribution to tumor subtype (59), suggesting age-associated luminal subtype breast cancers originate from more mature LEp. Signaling pathways, epigenetic regulation such as microRNAs and/or dysregulated genes influence the determination of distinct breast cancer subtypes (60). Indeed, age and the way cells bypass stress-associated stasis independently lead to distinct subtypes during the transformation from normal to immortal cells (61). *ELF5* is a key regulator for mature LEp and luminal progenitors. Therefore, decline of *ELF5* expression may affect maintenance of LEp lineage fidelity, and the resulting age-dependent cellular microenvironment is more conducive to cancer initiation.

Authors' Disclosures

R.W. Sayaman reports grants from NCI and NIH during the conduct of the study. B.L. Angarola reports grants, personal fees, and non-financial support from The Jackson Laboratory, grants from NIH and The V Foundation during the conduct of the study. O. Anczukow reports grants from V foundation, NIH, and The Jackson Laboratory during the conduct of the study. M.A. LaBarge reports grants from Department of Defense, NIH, Conrad N Hilton Foundation, and City of Hope during the conduct of the study; in addition, M.A. LaBarge has a patent for breast-specific risk predictor pending. No disclosures were reported by the other authors.

Authors' Contributions

M. Miyano: Conceptualization, data curation, formal analysis, funding acquisition, validation, investigation, visualization, methodology, writing—original draft, writing—review and editing. **R.W. Sayaman:** Conceptualization, data curation, formal analysis, funding acquisition, validation, visualization, writing—original draft, writing—review and editing. **S.F. Shalabi:** Investigation, writing—review and editing. **P. Senapati:** Data curation, investigation, visualization, writing—review and editing. **J.C. Lopez:** Investigation, writing—review and editing. **B.L. Angarola:** Formal analysis, investigation, visualization, writing—review and editing. **S. Hinz:** Data curation, writing—review and editing. **A. Zirbes:** Writing—review and editing. **O. Anczukow:** Formal analysis, funding acquisition, investigation, visualization, writing—review and

editing. **L.D. Yee:** Resources, writing–review and editing. **M.S. Sedrak:** Writing–review and editing. **M.R. Stampfer:** Resources, writing–review and editing. **V.L. Seewaldt:** Resources, writing–review and editing. **M.A. LaBarge:** Conceptualization, resources, supervision, funding acquisition, project administration, writing–review and editing.

Acknowledgments

We would like to acknowledge the contributions of our patient advocates, Susan Samson and Sandy Preto. Research reported in this publication included work performed in the Analytical Cytometry, Integrative Genomics and Bioinformatics, and Biomarker Analysis and Validation Cores supported by the NCI of the NIH under grant number P30CA033572. The content is solely the responsibility of the authors and does not necessarily represent the official views of the NIH. The results shown and referenced herein are in part based upon data generated by the TCGA Research Network. We are grateful for the generous support received from Phi Beta Psi Sorority, California (M. Miyano). The NIH: NCI, Cancer Metabolism Training Program Postdoctoral Fellowship T32CA221709 (R. Sayaman),

U01CA244109 and R01CA237602 (M.A. LaBarge); NIBIB R01EB024989 (M.A. LaBarge); NIA R33AG059206 (M.A. LaBarge); the Department of Defense/Army Breast Cancer Era of Hope Scholar Award BC141351 and Expansion Award BC181737, Conrad N. Hilton Foundation, and City of Hope Center for Cancer and Aging (M.A. La Barge). NIH grants P30CA034196 (O. Anczukow) and T32AG062409A (B. Angarola).

The publication costs of this article were defrayed in part by the payment of publication fees. Therefore, and solely to indicate this fact, this article is hereby marked “advertisement” in accordance with 18 USC section 1734.

Note

Supplementary data for this article are available at Cancer Prevention Research Online (<http://cancerprevres.aacrjournals.org/>).

Received December 9, 2020; revised April 29, 2021; accepted June 7, 2021; published first June 17, 2021.

References

- Ban KA, Godellas CV. Epidemiology of breast cancer. *Surg Oncol Clin N Am* 2014;23:409–22.
- Hiatt RA, Engmann NJ, Balke K, Rehkopf DH, Paradigm IIMP. A complex systems model of breast cancer etiology: the paradigm II conceptual model. *Cancer Epidemiol Biomarkers Prev* 2020;29:1720–30.
- Kuchenbaecker KB, Hopper JL, Barnes DR, Phillips KA, Mooij TM, Roos-Blom MJ, et al. Risks of breast, ovarian, and contralateral breast cancer for BRCA1 and BRCA2 mutation carriers. *JAMA* 2017;317:2402–16.
- Tung N, Lin NU, Kidd J, Allen BA, Singh N, Wenstrup RJ, et al. Frequency of germline mutations in 25 cancer susceptibility genes in a sequential series of patients with breast cancer. *J Clin Oncol* 2016;34:1460–8.
- Collaborative Group on Hormonal Factors in Breast C. Familial breast cancer: collaborative reanalysis of individual data from 52 epidemiological studies including 58,209 women with breast cancer and 101,986 women without the disease. *Lancet* 2001;358:1389–99.
- Benz CC. Impact of aging on the biology of breast cancer. *Crit Rev Oncol Hematol* 2008;66:65–74.
- Hernandez DG, Nalls MA, Gibbs JR, Arepalli S, van der Brug M, Chong S, et al. Distinct DNA methylation changes highly correlated with chronological age in the human brain. *Hum Mol Genet* 2011;20:1164–72.
- Christensen BC, Houseman EA, Marsit CJ, Zheng S, Wrensch MR, Wiemels JL, et al. Aging and environmental exposures alter tissue-specific DNA methylation dependent upon CpG island context. *PLoS Genet* 2009;5:e1000602.
- Hannum G, Guinney J, Zhao L, Zhang L, Hughes G, Sada S, et al. Genome-wide methylation profiles reveal quantitative views of human aging rates. *Mol Cell* 2012;49:359–67.
- Horvath S. DNA methylation age of human tissues and cell types. *Genome Biol* 2013;14:R115.
- Sehl ME, Henry JE, Storniolo AM, Ganz PA, Horvath S. DNA methylation age is elevated in breast tissue of healthy women. *Breast Cancer Res Treat* 2017;164:209–19.
- Johnson KC, Houseman EA, King JE, Christensen BC. Normal breast tissue DNA methylation differences at regulatory elements are associated with the cancer risk factor age. *Breast Cancer Res* 2017;19:81.
- Miyano M, Sayaman RW, Stoiber MH, Lin CH, Stampfer MR, Brown JB, et al. Age-related gene expression in luminal epithelial cells is driven by a microenvironment made from myoepithelial cells. *Aging* 2017;9:2026–51.
- Sayaman RW, Miyano M, Senapati P, Shalabi S, Zirbes A, Todhunter ME, et al. Epigenetic changes with age primes mammary luminal epithelia for cancer initiation. *bioRxiv* 2021:2021.02.12.430777.
- Labarge MA, Garbe JC, Stampfer MR. Processing of human reduction mammoplasty and mastectomy tissues for cell culture. *J Vis Exp* 2013;71:50011.
- Garbe JC, Bhattacharya S, Merchant B, Bassett E, Swisshelm K, Feiler HS, et al. Molecular distinctions between stasis and telomere attrition senescence barriers shown by long-term culture of normal human mammary epithelial cells. *Cancer Res* 2009;69:7557–68.
- Song MA, Brasky TM, Weng DY, McElroy JP, Marian C, Higgins MJ, et al. Landscape of genome-wide age-related DNA methylation in breast tissue. *Oncotarget* 2017;8:114648–62.
- Fortin JP, Triche TJ Jr, Hansen KD. Preprocessing, normalization and integration of the Illumina HumanMethylationEPIC array with minfi. *Bioinformatics* 2017;33:558–60.
- Johnson WE, Li C, Rabinovic A. Adjusting batch effects in microarray expression data using empirical Bayes methods. *Biostatistics* 2007;8:118–27.
- Garbe JC, Pepin F, Pelissier FA, Sputova K, Fridriksdottir AJ, Guo DE, et al. Accumulation of multipotent progenitors with a basal differentiation bias during aging of human mammary epithelia. *Cancer Res* 2012;72:3687–701.
- Piggin CL, Roden DL, Gallego-Ortega D, Lee HJ, Oakes SR, Ormandy CJ. ELF5 isoform expression is tissue-specific and significantly altered in cancer. *Breast Cancer Res* 2016;18:4.
- Lee HJ, Hinshelwood RA, Bouras T, Gallego-Ortega D, Valdes-Mora F, Blazek K, et al. Lineage specific methylation of the Elf5 promoter in mammary epithelial cells. *Stem Cells* 2011;29:1611–9.
- Ng RK, Dean W, Dawson C, Lucifero D, Madeja Z, Reik W, et al. Epigenetic restriction of embryonic cell lineage fate by methylation of Elf5. *Nat Cell Biol* 2008;10:1280–90.
- Jenkins EODA, Anders CK, Prat A, Perou CM, Carey LA, Muss HB. Age-specific changes in intrinsic breast cancer subtypes: a focus on older women. *Oncologist* 2014;19:1076–83.
- Kalyuga M, Gallego-Ortega D, Lee HJ, Roden DL, Cowley MJ, Caldon CE, et al. ELF5 suppresses estrogen sensitivity and underpins the acquisition of antiestrogen resistance in luminal breast cancer. *PLoS Biol* 2012;10:e1001461.

26. Voisin S, Harvey NR, Haupt LM, Griffiths LR, Ashton KJ, Coffey VG, et al. An epigenetic clock for human skeletal muscle. *J Cachexia Sarcopenia Muscle* 2020;11:887–98.
27. Hankinson SE, Willett WC, Colditz GA, Hunter DJ, Michaud DS, Deroo B, et al. Circulating concentrations of insulin-like growth factor I and risk of breast cancer. *Lancet North Am Ed* 1998;351:1393–6.
28. Key T, Appleby P, Barnes I, Reeves G, Endogenous H, Breast Cancer Collaborative G. Endogenous sex hormones and breast cancer in postmenopausal women: reanalysis of nine prospective studies. *J Natl Cancer Inst* 2002;94:606–16.
29. Gilley D, Tanaka H, Herbert BS. Telomere dysfunction in aging and cancer. *Int J Biochem Cell Biol* 2005;37:1000–13.
30. Sputova KGJ, Pelissier FA, Chang E, Stampfer MR, Labarge MA. Aging phenotypes in cultured normal human mammary epithelial cells are correlated with decreased telomerase activity independent of telomere length. *Genome Integr* 2013;4:4.
31. Ahuja N, Li Q, Mohan AL, Baylin SB, Issa JP. Aging and DNA methylation in colorectal mucosa and cancer. *Cancer Res* 1998;58:5489–94.
32. Levine ME, Lu AT, Quach A, Chen BH, Assimes TL, Bandinelli S, et al. An epigenetic biomarker of aging for lifespan and healthspan. *Aging* 2018;10:573–91.
33. Lu AT, Quach A, Wilson JG, Reiner AP, Aviv A, Raj K, et al. DNA methylation GrimAge strongly predicts lifespan and healthspan. *Aging* 2019;11:303–27.
34. Weidner CI, Lin Q, Koch CM, Eisele L, Beier F, Ziegler P, et al. Aging of blood can be tracked by DNA methylation changes at just three CpG sites. *Genome Biol* 2014;15:R24.
35. Hofstatter EW, Horvath S, Dalela D, Gupta P, Chagpar AB, Wali VB, et al. Increased epigenetic age in normal breast tissue from luminal breast cancer patients. *Clin Epigenetics* 2018;10:112.
36. Hoffman A, Pellenberg R, Drendall CI, Seewaldt V. Comparison of random periareolar fine needle aspirate versus ductal lavage for risk assessment and prevention of breast cancer. *Curr Breast Cancer Rep* 2012;4:180–7.
37. Falandry C, Bonnefoy M, Freyer G, Gilson E. Biology of cancer and aging: a complex association with cellular senescence. *J Clin Oncol* 2014;32:2604–10.
38. Hubbard JM, Cohen HJ, Muss HB. Incorporating biomarkers into cancer and aging research. *J Clin Oncol* 2014;32:2611–6.
39. Lara J, Cooper R, Nissan J, Ginty AT, Khaw KT, Deary IJ, et al. A proposed panel of biomarkers of healthy ageing. *BMC Med* 2015;13:222.
40. Margolick JB, Ferrucci L. Accelerating aging research: how can we measure the rate of biologic aging? *Exp Gerontol* 2015;64:78–80.
41. Wildiers H, Heeren P, Puts M, Topinkova E, Janssen-Heijnen ML, Extermann M, et al. International Society of Geriatric Oncology consensus on geriatric assessment in older patients with cancer. *J Clin Oncol* 2014;32:2595–603.
42. Soto-Perez-de-Celis E, Li D, Yuan Y, Lau YM, Hurria A. Functional versus chronological age: geriatric assessments to guide decision making in older patients with cancer. *Lancet Oncol* 2018;19:e305–e16.
43. Mohile SG, Dale W, Somerfield MR, Schonberg MA, Boyd CM, Burhenn PS, et al. Practical assessment and management of vulnerabilities in older patients receiving chemotherapy: ASCO Guideline for Geriatric Oncology. *J Clin Oncol* 2018;36:2326–47.
44. Mohile SG, Velarde C, Hurria A, Magnuson A, Lowenstein L, Pandya C, et al. Geriatric assessment-guided care processes for older adults: a Delphi consensus of geriatric oncology experts. *J Natl Compr Canc Netw* 2015;13:1120–30.
45. Stute P, Sielker S, Wood CE, Register TC, Lees CJ, Dewi FN, et al. Life stage differences in mammary gland gene expression profile in non-human primates. *Breast Cancer Res Treat* 2012;133:617–34.
46. Ma XJ, Salunga R, Tuggle JT, Gaudet J, Enright E, McQuary P, et al. Gene expression profiles of human breast cancer progression. *Proc Natl Acad Sci U S A* 2003;100:5974–9.
47. Chakrabarti R, Wei Y, Romano RA, Decoste C, Kang Y, Sinha S. Elf5 regulates mammary gland stem/progenitor cell fate by influencing notch signaling. *Stem Cells* 2012;30:1496–508.
48. Chakrabarti R, Hwang J, Andres Blanco M, Wei Y, Lukacis M, Romano R-A, et al. Elf5 inhibits the epithelial–mesenchymal transition in mammary gland development and breast cancer metastasis by transcriptionally repressing Snail2. *Nat Cell Biol* 2012;14:1212–22.
49. Singh S, Kumar S, Srivastava RK, Nandi A, Thacker G, Murali H, et al. Loss of ELF5-FBXW7 stabilizes IFNGR1 to promote the growth and metastasis of triple-negative breast cancer through interferon-gamma signalling. *Nat Cell Biol* 2020;22:591–602.
50. Osako T, Lee H, Turashvili G, Chiu D, McKinney S, Joosten SEP, et al. Age-correlated protein and transcript expression in breast cancer and normal breast tissues is dominated by host endocrine effects. *Nat Cancer* 2020;1:1–15.
51. Zheng L, Annab LA, Afshari CA, Lee WH, Boyer TG. BRCA1 mediates ligand-independent transcriptional repression of the estrogen receptor. *Proc Natl Acad Sci U S A* 2001;98:9587–92.
52. Lim E, Vaillant F, Wu D, Forrest NC, Pal B, Hart AH, et al. Aberrant luminal progenitors as the candidate target population for basal tumor development in BRCA1 mutation carriers. *Nat Med* 2009;15:907–13.
53. Mavaddat N, Barrowdale D, Andrulis IL, Domchek SM, Eccles D, Nevanlinna H, et al. Pathology of breast and ovarian cancers among BRCA1 and BRCA2 mutation carriers: results from the consortium of investigators of modifiers of BRCA1/2 (CIMBA). *Cancer Epidemiol Biomarkers Prev* 2012;21:134–47.
54. Cybulski C, Kluźniak W, Huzarski T, Wokołoczyk D, Kashyap A, Jakubowska A, et al. Clinical outcomes in women with breast cancer and a PALB2 mutation: a prospective cohort analysis. *Lancet Oncol* 2015;16:638–44.
55. Zhang F, Fan Q, Ren K, Andreassen PR. PALB2 functionally connects the breast cancer susceptibility proteins BRCA1 and BRCA2. *Mol Cancer Res* 2009;7:1110–8.
56. Piggini CL, Roden DL, Law AMK, Molloy MP, Krisp C, Swarbrick A, et al. ELF5 modulates the estrogen receptor cistrome in breast cancer. *PLoS Genet* 2020;16:e1008531.
57. Van Keymeulen A, Lee MY, Ousset M, Brohee S, Rorive S, Girardi RR, et al. Reactivation of multipotency by oncogenic PIK3CA induces breast tumour heterogeneity. *Nature* 2015;525:119–23.
58. Proia TA, Keller PJ, Gupta PB, Klebba I, Jones AD, Sedic M, et al. Genetic predisposition directs breast cancer phenotype by dictating progenitor cell fate. *Cell Stem Cell* 2011;8:149–63.
59. Pommier RM, Sanlaville A, Tonon L, Kielbassa J, Thomas E, Ferrari A, et al. Comprehensive characterization of claudin-low breast tumors reflects the impact of the cell-of-origin on cancer evolution. *Nat Commun* 2020;11:3431.
60. Zhou J, Chen Q, Zou Y, Chen H, Qi L, Chen Y. Stem cells and cellular origins of breast cancer: updates in the rationale, controversies, and therapeutic implications. *Front Oncol* 2019;9:820.
61. Lee JK, Garbe JC, Vrba L, Miyano M, Futscher BW, Stampfer MR, et al. Age and the means of bypassing stasis influence the intrinsic subtype of immortalized human mammary epithelial cells. *Front Cell Dev Biol* 2015;3:13.